A MULTI-SCALE MATERIALS MODELING METHOD WITH SEAMLESS ZOOMING CAPABILITY BASED ON SURFACELETS

Wei Huang
HP Labs
Palo Alto, CA, 94304
huang@hp.com

Yan Wang*
School of Mechanical Engineering
Georgia Institute of Technology
Atlanta, GA, 30332
yan.wang@me.gatech.edu

David W. Rosen
School of Mechanical Engineering
Georgia Institute of Technology
Atlanta, GA, 30332
david.rosen@me.gatech.edu

* corresponding author. Tel. +1-404-894-4714 Fax. +1-404-894-9342

o An earlier version of this paper was presented at 2014 IDETC/CIE Conference as DETC2014-34435.

A MULTI-SCALE MATERIALS MODELING METHOD WITH SEAMLESS ZOOMING CAPABILITY BASED ON SURFACELETS

ABSTRACT

In multi-scale materials modeling, it is desirable that different levels of details can be specified in different regions of interest without the separation of scales so that the geometric and physical properties of materials can be designed and characterized. Existing materials modeling approaches focus more on the representation of the distributions of material compositions captured from images. In this paper, a multi-scale materials modeling method is proposed to support interactive specification and visualization of material microstructures at multiple levels of details, where designer's intent at multiple scales is captured. This method provides a feature-based modeling approach based on a recently developed surfacelet basis. It has the capability to support seamless zoom-in and zoom-out. The modeling, operation, and elucidation of materials are realized in both the surfacelet space and the image space.

Keywords: Materials modeling; Surfacelet; Surfacelet transform

1. INTRODUCTION

Nanotechnology enables engineers to create or modify details of materials at nano-scales so as to realize more desirable material properties. As this technology becomes more pervasive, it is foreseen that some materials modeling modules will be embedded in future computer-aided design systems so that the geometry and materials of a product can be designed concurrently. The core research issue of materials design is to establish process–structure–property (PSP) relations and search optimum solutions to achieve desirable properties. The models of microstructures and compositions in materials thus are essential to allow for quantification of PSP relations. Because the overall material properties can be affected by the details of microstructures and compositions at all scales, these material models should support specification at multiple length scales. Here, the term microstructure does not particularly refer to the internal material structures at the micrometer scale only, but to those at any scales that are suitable for describing material distributions. The design of material microstructure forms the basis for the design of material compositions. As the material microstructure defines the 'skeleton' or major material distributions, the material composition is more like the 'flesh and skin' in addition to the microstructural information. That is, compositions depend on structures. Take the fiber-based composite as an example. The positions and orientations of the fibers define the microstructure and outline the overall distribution of materials, whereas the material composition information in the regions of fibers, matrix and the fiber-matrix interphases follow the overall trend defined by the fiber microstructures. In traditional

bulk-scale geometric modeling, features are widely used to define geometries. In the domain of material microstructures, microstructures also show some patterns. Therefore, most of the microstructural information can be modeled by highlighting these patterns. We call these patterns *microstructural features*. The microstructural features are important in determining the material properties. Thus, how to effectively utilize microstructural features in materials design is a key issue of multi-scale materials modeling.

Different from the classic geometric modeling, microstructural modeling uses digital material images as the essential medium for both design and reverse engineering processes. Images from material microstructures (optical or scanning electron microscope) contain the most comprehensive information about the materials. They also provide visualization of materials for engineers. Traditionally two- or three-dimensional (3D) material images are used to directly generate tessellation or mesh representation of microstructural geometries such as composites [1], crystals [2], or defects [3] for finite element simulation and property prediction. Yet, this reverse engineering approach focuses on the representation of stochastic distributions of phases in existing materials, instead of the specification of desirable compositions. Some shape descriptor based approaches have been developed to represent material phase distributions, such as spatial correlation with point statistics [4,5]. These descriptors provide stochastic approaches to specify non-deterministic microstructures. To the authors' best knowledge, there is no mechanism of microstructural modeling that supports multi-scale materials specification. A material model that captures designer's intent at multiple scales and integrates image-based visualization is needed for designers to generate their design concepts during the specification process.

Here, we propose a new multi-scale materials specification scheme based on material images and microstructural feature modeling. In such a multi-scale specification environment, a design engineer will be able to specify material microstructures, compositions and properties at certain regions of interest. Most importantly, the proposed materials modeling mechanism for design has a seamless zoom-in and zoom-out capability such that material information at multiple scales can be exchanged without artificial separations of scales. In this environment, a user can specify the values of microstructural properties at certain locations in the region of interest. The property distribution within the domain can then be created from the specifications based on interpolation mechanisms. If the user would like to inspect the modeled materials in a specific region with finer details, he or she can perform a zoom-in operation. A smaller scale model of the region will be generated based on his or her specifications. To show the effect in a larger region as a result of the specification procedure, a zoom-out operation can be performed.

The proposed materials specification scheme is based on a recently developed surfacelet transform [6]. A forward surfacelet transform enables the representation of material microstructures by effectively capturing microstructural features from material images. An inverse surfacelet transform that reconstructs material images from the surfacelet model was also developed [7]. In the surfacelet based materials design environment, the designer can perform design specifications in both image (real) space and surfacelet (reciprocal)

space. Images are commonly used as the medium in materials design and characterization. Thus, we use images to visualize our specified material distributions. The image representation of materials in the image space is called *visualization model*. Surfacelet space, on the other hand, is used for the ease of specifying microstructural features. The values in surfacelet space and the pixel values in image space contain the same information of material distributions. Image space has three dimensions (x, y, and z), whereas the dimensions of surfacelet space correspond to the number of shape, orientation, and position parameters, which will be introduced in details in Section 2.2. The most of design specification procedure is done in the surfacelet space. A user can specify the values of microstructures, compositions, or properties at discrete locations or called *collocation points* in the region of interest within the surfacelet space. The local property distribution within the domain can then be created based on a continuous *distribution model*, which is the result of interpolation from the specification. The visualization model in the image space is an evaluation of the distribution model in the surfacelet space for a particular image resolution. Since the collocation points could be selected at any locations based on the designer's need, whereas regular spacing is required to generate the interpolated distribution model, a regular grid in the region of interest will be generated based on the collocation points. The regularly generated locations on the grid are called *grid points*. Some of the grid points are the specified collocation points. The additional grid points are generated from the collocation points by interpolation or extrapolation. The general procedure of a material specification process is shown in Figure 1, and descried as follows.

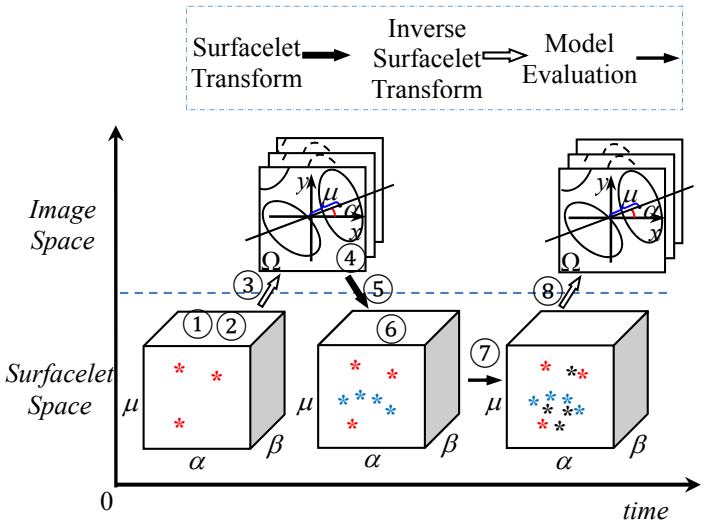

Figure 1 The general procedure of materials specification

(1) The designer chooses appropriate types and shape parameters of surfacelets to represent the geometry of the desired microstructural features. (2) Some collocation points are specified in the surfacelet space to represent the features. (3) The material

distributions then are generated in the image space accordingly. (4) Additional features are specified in the image space. The specification in the surfacelet space provides the basic feature information that quickly creates the distribution. Yet, some special artifacts such as impurity, defects, and discontinuity cannot be specified easily in the surfacelet space. Therefore, the use of the image space for specification is also necessary. (5) After the specification of the special artifacts, a surfacelet transform can generate the corresponding specification in the surfacelet space. The special artifacts in the surfacelet space after the surfacelet transform may be continuous and represented by many discrete collocation points in the implementation. (6) With the specified collocation points, the grid and grid points are generated. (7) The continuous distribution model then is created by interpolation. (8) The final specification in the image space is generated by the inverse surfacelet transform from the evaluated distribution model in the surfacelet space.

If the user would like to inspect the modeled materials in a specific region with finer details, he or she can perform a zoom-in operation. A smaller scale model of the region will be generated based on his or her specifications. To show the effect in a larger region as a result of the design procedure, a zoom-out operation can be performed. The operation is straight-forward. Some collocation points will be selected to generate a coarser-grid interpolation model at a larger scale. Therefore, compared to zoom-out, the zoom-in operation is more complex in a multi-scale modeling method.

Because the surfacelets created for the main microstructural features at the beginning of the specification process can not only be specified by users from scratches, but also be obtained from the forward surfacelet transform of existing material images, the proposed multi-scale materials modeling method is also applicable in a re-engineering process where existing materials is re-designed by adding more specifications.

In the remainder of the paper, the related work is discussed in Section 2. The collocation technique developed for the zoom-in operation is introduced in Section 3. In Section 4, the detailed multi-scale materials specification process is described in details. An example of specification for fiber-based composite is used to demonstrate the new specification process in Section 5. The conclusion and planned future work will be given in Section 6.

2. RELATED WORK

2.1 Shape descriptions of material microstructures

The purpose of the proposed multi-scale materials specification method in this paper is for the ease of structure–property relation construction, by using a feature-based interactive microstructural modeling approach with descriptors. Different shape descriptors have been developed to characterize the phase and microstructural distributions in heterogeneous materials. For particle reinforced composites, the variance of mean near-neighbor distances for particles [8,9] was proposed to characterize heterogeneity of distributions.

Morphological shape descriptors such as area, perimeter, roundness, and smoothness [10], and topological descriptors as Minkowski functionals [11] were used. In constructing structure–property relations, statistical distributions of material microstructures were represented with spherical harmonics for one-point crystal orientation distribution function [12] and two-point spatial correlation function as the probability that material composition at two locations belong to certain phases [13,14] to capture polycrystalline or anisotropic materials information. A similar statistical descriptor is the two-point cluster function as the probability that two points fall into the same cluster [15,16]. To extract two-point statistical descriptors, the straightforward method is using Monte Carlo sampling [17,18]. A more efficient approach is based on fast Fourier transform [19]. Higher-order N-point correlation functions can be calculated from lower-order ones [20]. Based on statistical correlation descriptors, structure-property relationship can be established for design [21,22,23].

The above methods extract statistical information of microstructures based on material images. Limited research is done to generate 3D material structures systematically. Wu et al. [24] proposed a Markov chain method to generate voxels of stochastic porous media. Wang et al. [25,26,27,28,29] proposed analytical models of triply periodic minimal surfaces (TPMS) to represent porous material structures. Jung et al. [30] proposed an optimization based approach to build TPMS. Yoo [31,32] and Afshar et al. [33] applied TPMS in modeling porous scaffold. Didari et al. [34] used TPMS to model structures of fibrous porous media. Yang et al. [35] used stochastic TPMS in constructing porous scaffold. Xiao and Yin [36] modeled random structures of porous media using Voronoi tessellations. Fractals were also used to model the irregularity of surfaces in porous materials and fracture surfaces [37,38,39].

The modeling method proposed in this paper is to provide a multi-scale microstructural modeling based on the concept of surfacelets [6] for design specification in an interactive design environment. The surfacelet, surfacelet transform, and inverse surfacelet transform will be introduced in Section 2.2.

2.2 Surfacelet, surfacelet transform and inverse surfacelet transform

A new dual-Rep modeling approach was recently proposed for heterogeneous materials modeling [6]. It is able to construct geometric boundaries and internal material distributions at the same time. The core component of this representation is based on a new basis function, called surfacelet. The surfacelet-based modeling approach enables us to capture material distributions at multiple scales. Three examples of surfacelets, 3D ridgelet, cylindrical surfacelet (or cylinderlet), and ellipsoidal surfacelet (or ellipsoidlet), are respectively defined as follows.

A 3D ridgelet that represents planar singularities is defined as

$$\psi_{a,\mu,\alpha,\beta}(\mathbf{r}) = a^{-1/2}\varphi\left(a^{-1}\left(\cos\beta\cos\alpha\cdot x+\cos\beta\sin\alpha\cdot y+\sin\beta\cdot z-\mu\right)\right)$$

A cylindrical surfacelet is defined as

$$\psi_{a,\mu,\alpha,\beta,r_1,r_2}(\mathbf{r}) = a^{-1/2}\varphi\left(a^{-1}[r_1(\cos\beta\cos\alpha\cdot x+\cos\beta\sin\alpha\cdot y+\sin\beta\cdot z-\mu)^2+r_2(-\sin\alpha\cdot x+\cos\alpha\cdot y)^2]\right) \quad (1)$$

And an ellipsoidal surfacelet is defined as

$$\psi_{a,\mu,\alpha,\beta,r_1,r_2,r_3}(\mathbf{r}) = a^{-1/2}\varphi\left(a^{-1}\begin{bmatrix} r_1(\cos\beta\cos\alpha\cdot x+\cos\beta\sin\alpha\cdot y+\sin\beta\cdot z-\mu)^2 \\ +r_2(-\sin\alpha\cdot x+\cos\alpha\cdot y)^2 \\ +r_3(-\sin\beta\cos\alpha\cdot x+\sin\beta\sin\alpha\cdot y+\cos\beta\cdot z)^2 \end{bmatrix}\right)$$

where $\mathbf{r}=(x, y, z)$ is the location in the Euclidean space, φ is a wavelet function, r_1, r_2 and r_3 are shape parameters that are fixed during transformation, α and β are orientation parameters, a is the scale parameter, and μ is the position parameter. The geometric interpretations of the isosurfaces for the three surfacelets for planar, cylindrical, and ellipsoidal singularities are shown in Figure 2. More complex surfacelets can be constructed from simple ones [40].

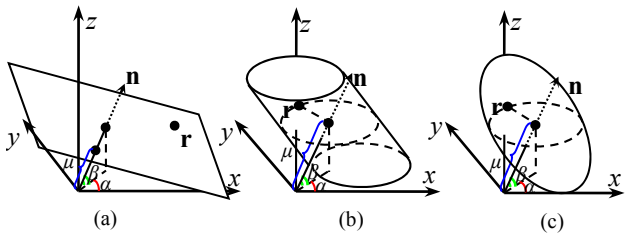

Figure 2 Geometric interpretation of surfacelets. (a) 3D Ridgelet; (b) Cylindrical surfacelet; (c) Ellipsoidal surfacelet

The reverse engineering method to construct the surfacelet model directly from material images was developed. This construction of the surfacelet model is called surfacelet transform. From a 3D material image, the values of surface integrals on surfacelets are calculated by summing up the pixel values on the isosurfaces of surfacelets and arranged in a 3D matrix with orientation and position parameters α, β, and μ as indices. The orientation and position parameters form the surfacelet space. Then 1D wavelet transforms along the μ axis direction can be performed for all α's and β's for compression purpose. The results are surfacelet coefficients for a particular angle and position of the surfacelet. In general, the dimension of the transformed space or surfacelet space corresponds to the number of orientation and position parameters used in the surfacelet. The surfacelet space can be also extended to include shape parameters such as the radii of cylinders and ellipsoids. The material images can also be reconstructed from surfacelet coefficients with the inverse surfacelet transform [7].

3. THE COLLOCATION METHOD FOR ZOOM-IN OPERATION

3.1 Interpolation and extrapolation in the surfacelet space

The collocation method proposed here is to efficiently use the specified collocation points for interpolation at different scales. In a multi-scale modeling environment, interpolation and extrapolation are conducted based on the collocation points at different scales to generate necessary grid points in the surfacelet space. A continuous distribution model is an interpolation from the grid points. Therefore, the representation of the material distribution based on the collocation method is efficient. Although collocation in the image space is possible in implementing a multi-scale modeling environment, it is not efficient in capturing material distributions because the pixel values representing microstructural and compositional information are independent from each other, and the interpolation or extrapolation of pixel values loses the feature information. In contrast, the interpolation or extrapolation in the surfacelet space retains feature information and provides good continuity. The idea is to predict the surface integral values in a domain from some specified ones with an interpolation model. Adjacent surfacelets have some pixels in common, and therefore their surface integral values are correlated. The interpolation thus can have good accuracy. In the interpolation model, surface integral values are functions of position and orientation parameters. Some surfacelets with selected positions and orientations are used to predict the others based on the interpolation model.

In this paper, an example 3D image of fiber-based composite, as shown in Figure 3, is utilized for the demonstration of our approach. Here it is also used to demonstrate interpolation and extrapolation in the surfacelet space.

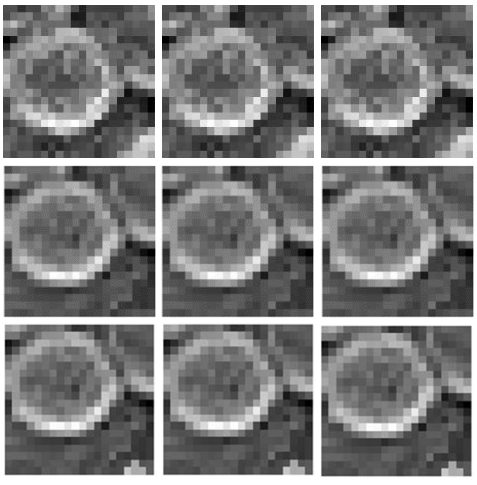

Figure 3 An example 3D image of fiber-based composite

To illustrate the interpolation in the surfacelet space, a surfacelet transform is first applied to the images in Figure 3. The cylindrical

surfacelet in Eq.(1) is applied. The ranges of the orientation parameters are set to be $\mu \in (0, D/2) = (0, 1.73)$, $\alpha \in [0, 2\pi)$ and $\beta \in [-\pi/2, \pi/2]$ to ensure that the surfacelets cover all of the pixels, where $D = \sqrt{2^2 + 2^2 + 2^2}$ is the diagonal length of the 3D images. The 1D and 2D interpolations are described as follows.

3.1.1 1D interpolation in the surfacelet space

Suppose that the numbers of discretized μ, α, and β are u, f, and g respectively. The number of specified surfacelets in the surfacelet space is $Q = u \times f \times g = 11 \times 11 \times 3$. As shown in Figure 4, a cubic spline interpolation is applied to predict surface integral values with respect to rotational angle α, where β=−π/90 and μ=0. In the figure, stars ('*') indicate the surface integral values I for the specified collocation points in the surfacelet space. The interpolated function $I(\alpha)$ is then used to predict the values of some new surface integrals. The dots in the figure are the actual surface integral values calculated with more surfacelets in the surfacelet transform where $Q = u \times f \times g = 22 \times 22 \times 3$. The stars and dots are evenly spaced. The result shows that the prediction is reasonably well.

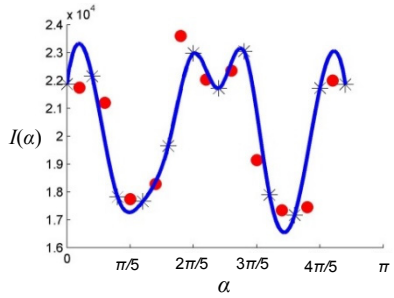

Figure 4 Result of Cubic spline interpolation for parameter α

With the same β and μ values, the result of piecewise cubic Hermite interpolation for parameter α is shown in Figure 5. It can be seen that the piecewise cubic Hermite method has better interpolation result than the cubic spline method, although the cubic spline curve is smoother.

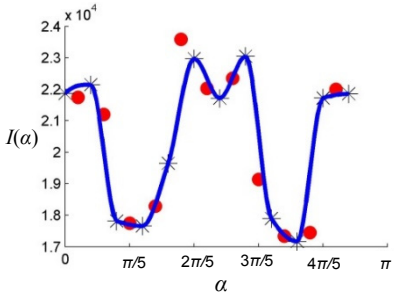

Figure 5 Result of piecewise cubic Hermite interpolating polynomial for parameter α

When interpolation is performed along the translation direction μ, the result of the cubic spline interpolation for parameter μ is shown in Figure 6, where α=0 and β=−π/90.

3.1.2 2D interpolation in the surfacelet space

When the interpolation for both rotation and translation is applied, the result of the cubic spline interpolation for parameters α and μ is shown in Figure 7, where β=−π/90, the stars denote the specified ones, and the dots are the ones to predict.

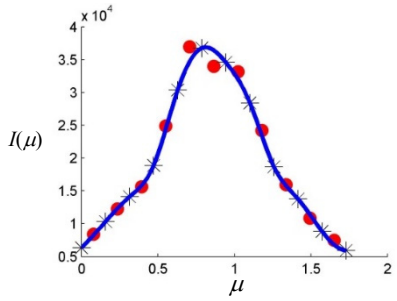

Figure 6 Result of cubic spline interpolation for parameter μ

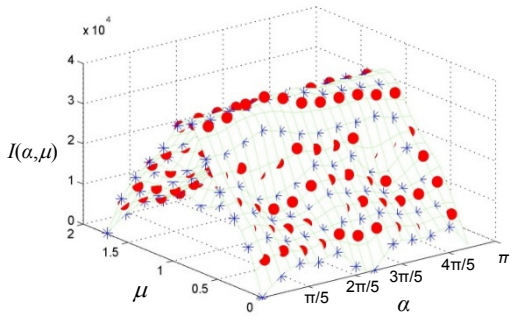

Figure 7 Result of 2D cubic spline interpolation for parameter μ and α

From the results of both 1D and 2D interpolation, it can be seen that the true surface integral values can be predicted from the specified collocation points reasonably well. The interpolation provides good prediction without losing feature information. Throughout the process, the information of spatial correlation among pixels that form the feature is maintained.

3.2 Collocation for zoom-in and zoom-out operations

In this subsection, the proposed collocation method for zoom-in and zoom-out operations is described. The proposed method is

general enough for all interpolation or extrapolation basis functions. Here, the general principle is illustrated by 1D and 2D cases.

3.2.1 Collocation grid

From user-specified data points in the surfacelet space, a regular collocation grid needs to be determined such that the spatial relationship of the data points is determined, and spatially organized collocation points can be generated for interpolation. The grids represent levels of data, whereas the collocation points are selected for interpolation and extrapolation at different levels. The general rule of grid generation is that grids should be oriented to cover all collocation points in the domain but with the smallest grid area. The subdivision pattern used to generate multi-level grids used in this paper is bi-sectional, although other patterns can also be applied for the proposed zoom operations.

A 1D example of the bi-section collocation scheme is shown in Figure 8(a), and a 2D case is shown in Figure 8(b). In Figure 8(a), stars ('*') represent the first-level collocation points, and the circle ('o') represents the second-level collocation point between the two first-level collocation points. For the 2D case in Figure 8(b), the grid is formed at different levels according to the collocation points, which are used in the zoom operation. The collocation points of the first level are predetermined, which are the four corner points in the whole domain. The point located at the middle of the line formed by two first-level collocation points, as the result of bi-section, is at the second level. Similarly, the point at the middle of the line formed by a pair of second-level collocation points is at the third level. It is possible that the collocation points cannot be categorized in adjacent levels, such as the example in Figure 8(b) where no collocation points are at level 2. When a point is specified in the surfacelet space, the level where the collocation point belongs to can be determined by calculating the distance between the collocation point and some close-by grid points. When a collocation point has a distance to a grid point that is within a given tolerance, it is moved to the corresponding grid point as the quantization to reduce the total number of levels in the problem.

3.2.2 Zoom-in operation

For a material region where the user is interested in specifying the details, a zoom-in operation is conducted. The zoom-in operation is realized by interpolation in the surfacelet space. For the interpolation, three adjacent levels of collocation points are needed to ensure the smoothness of zoom-in operation. At the lowest level among the three used in the zoom-in operation, a complete set of grid points in the region of interest is required for the operation. If the values of some of the grid points are missing, extrapolation from other known grid points is needed. The extrapolation procedure is illustrated in Figure 9(a). The original collocation points correspond to the value pairs at P_1=[0, 0], P_2=[0.5, 0.25], P_3=[0.625, 0.39], and P_4=[0.75, 0.5625], where the first value is the x coordinate and the second one is its surface integral value $I(x)$. The first-level grid points are those at x=0.5N, where N is an integer, such as P_1 and P_2. The second-

level grid points include the first-level ones as well as those grid points between the first-level ones by bi-section, such as P_1, P_2, and P_4. Similarly, the third-level grid points include the first-level, second-level, as well as those between the second-level grid points, such as P_1, P_2, P_3, and P_4. To zoom into the sub region of $x \in [0.5,1]$, a new grid point P_5 at x=1 is needed. The surface integral value of P_5 is estimated by extrapolation from P_1, P_2, and P_4. In this example, a cubic spline is used. The result P_5=[1,1] is obtained. Then P_2, P_3, P_4, and P_5 are utilized to generate an interpolation model that can be used to describe other intermediate points in the region of $x \in [0.5,1]$. The interpolation is the resulting model after the zoom-in operation. Similarly, a 2D example is shown in Figure 9(b). Notice that extrapolation is always conducted based on the data points on two adjacent levels of grid points, and the extrapolated grid points are always on the lower level grid.

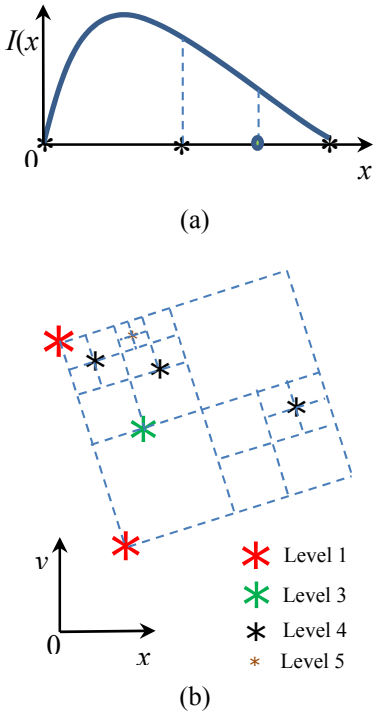

Figure 8 Determination of the levels of collocation points. (a) 1D collocation. (b) 2D collocation.

3.2.3 Zoom-out operation

After the user specifies the detailed material information at small scales with the zoom-in operation, the user usually wants to zoom out to check the overall microstructure and material distribution, or move to another region to perform the zoom-in operation. In the

zoom-out operation, there are two approaches to create grid points of a larger scale model. The first approach is to choose some existing grid points that also belong to a smaller scale so that the larger scale model can be generated. The second approach is a homogenization approach where the surface integral value at a grid point of the larger scale is the average of the values at some adjacent grid points in the smaller scale model. After the grid points of the larger scale model are chosen, the interpolation scheme is applied to predict any unknown position following the same procedure in the zoom-in operation. For instance, in Figure 9(a), if the user wants to visualize the entire material domain, the grid points P_1, P_2, and P_5 can be chosen for a larger scale model from the original small one. The larger scale model is the interpolated model based on P_1, P_2, and P_5.

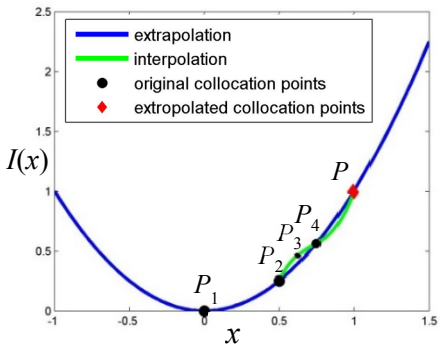

(a)

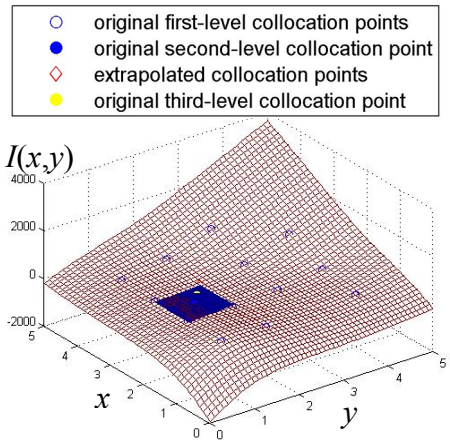

(b)

Figure 9 1D and 2D zoom-in examples. (a) 1D zoom-in. (b) 2D zoom-in.

4. MULTI-SCALE MATERIALS MODELING PROCESS

4.1 The combination of the material model and the visual zoom-in and zoom-out operations

Here we differentiate visual zoom operations from the material model zoom operations. During the material model zoom operations in the surfacelet space, the underlying material distribution models are created or modified. In contrast, the zoom operations in the image space only provide different visualization models without affecting the distribution models in the surfacelet space.

Because the size of 3D material images is usually large, in order to improve computational efficiency, it is desirable to use images with the resolution as low as possible in the design process. During the visual zoom-in and zoom-out operations, images at different visual scales have the same underlying material distribution model in the surfacelet space, although more pixels may be shown for a region of interest with more detailed material information to be visualized. The visual zoom-in and zoom-out operations can be simply conducted through changing the image resolution and re-evaluating the underlying material distribution model in the surfacelet space.

4.2 Detailed modeling and specification steps

The general procedure of the multi-scale modeling and specification process is shown in Figure 1. The detailed steps are listed in Figure 10 and descried as follows.

In Step 1, appropriate types and shape parameters of surfacelets are decided to represent the geometry of the microstructural features. The determined surfacelet forms affect the data exchange between the image space and surfacelet space. It should be noted that the type of the surfacelet is not limited to the existing surfacelet primitives. It can also be composite surfacelets that are combined with those surfacelet primitives for more complex features.

In Step 2, the location and orientation of a feature are specified as a point in the surfacelet space. Once the type and size of a surfacelet are determined, a microstructural feature in the image space can then be created based on the specified point in the surfacelet space. This makes the design process easier and more accurate than directly creating features in the image space.

In Step 3, the visualization model in the 3D material image space can be obtained through the inverse surfacelet transform of the intermediate result from Step 2 in the surfacelet space. Since only the boundaries need to be reconstructed, the general optimization based approach for the inverse surfacelet transform [7] is not necessarily applied. Instead, a simple scheme that set the pixels on the boundaries to be equal can be used.

In Step 4, more detailed material microstructural information, i.e. special artifacts, is specified in the image space across different visual scales. The microstructural information specified at this step is usually irregular, such as cracks or impurities, which are not efficient to be specified in the surfacelet space.

In Step 5, the forward surfacelet transform is applied so that the surfacelet representation of the resulting material images from Step 4 is obtained.

In Step 6, the interpolation or extrapolation is applied to build the grid based on the specified collocation points from Step 5. The continuous material distribution model is then constructed in the surfacelet space.

In Step 7, the continuous distribution model constructed in Step 6 is evaluated first in the surfacelet space so that the desirable resolution is obtained by introducing more surfacelets.

In Step 8, the inverse surfacelet transform is applied to the evaluated distribution model in the surfacelet space and the final material distribution as the result of specification process is obtained in the image space.

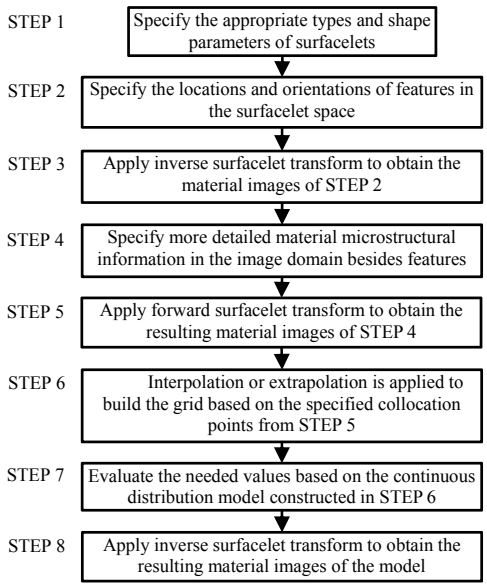

Figure 10 The general procedure of the computer-aided material microstructure modeling and specification process

If zoom-in or zoom-out operations are needed, the above eight-step specification process can be repeatedly applied. Based on the zoom procedures in Sections 3.2, new specified collocation points in the new scale are obtained. Then these collocation points in the surfacelet space will be used as the initial specification for Step 1 of the above process. The zoom-in and zoom-out operations can be applied repeatedly.

5. EXAMPLES AND RESULTS

In this section, an example of fiber-based composites is used to demonstrate the proposed multi-scale materials specification method. In this example, a representative volumetric element (RVE) of the fiber composite is used, which contains three fibers with different locations and orientations. The composite has three regions: the fiber, the matrix, and the fiber-matrix interphase. The interphase

is the gradient mixture between the fiber and matrix materials in the fiber boundaries. Both the fiber and the matrix materials are homogeneous. The fiber-matrix interphase is also of the interest for multi-scale material specification in addition to the fiber and the matrix. In this example, all images that show the intermediate results during the design specification process have the same resolution. The image size is chosen as 20×20×9 pixels. The origin of the image space is at the middle of the 3D image. The size of the image domain is $x, y, z \in [-1,1]$ for all visual scales.

In the first step, the shape parameters of the fibers are specified. In this example, the only shape parameters, which are the radii of fibers, are set to be 0.5. It should be noted that this number is proportional to the image domain, which is [-1,1] for all x, y, and z directions.

In the second step, the locations and orientations of the three fibers are specified in the surfacelet space. As discussed in Section 2.2, the dimension of the surfacelet space generally corresponds to the number of orientation and position parameters used in the surfacelets. However, for this example, the fourth parameter, the radius r, is introduced as the shape parameter in addition to α, β, and μ in order to model the gradient of the interphase region.

In this example, the size of the surfacelet domain is $u \times f \times g \times s = 30 \times 30 \times 4 \times 6$. The ranges of the orientation parameters are set to be $\mu \in (0, D/2) = (0,1.73)$, $\alpha \in [0, 2\pi)$, $\beta \in [-\pi/2, \pi/2]$ and $r \in [0,3]$ to ensure that the surfacelets cover all of the possible surfacelet positions and orientations, where $D = \sqrt{2^2 + 2^2 + 2^2}$ is the diagonal length of the 3D images. The user specified coordinates for the three collocation points in the surfacelet space are [0.692, 1.257, 0.5], [1.386, 1.885, 0.5], and [0.693, 4.398, 0.5], or at the indices of [12, 6, 6], [24, 9, 6], and [6, 21, 6] respectively. They are shown in Figure 11. The surfacelet space is 4D. Because the three fibers have the same parameter value of β, only the subspace of α, μ, and r is shown in the figure. The three collocation points have the same value for parameter r, which indicates that the three surfacelets have the same radius.

In the third step, by the inverse surfacelet transform, the 3D material images can be obtained. The pixel values on the boundaries are set to be equal. In this example, all pixel values are set to be 255.The result is shown in Figure 12. To show the contrast with the result in a higher resolution (more discrete values in the image space), an image with the resolution of 50×50×9 with the same material model is shown in Figure 13. It can be seen from Figure 13 that the position and orientation, as well as the boundary information of the fibers is visually very clear. In contrast, in Figure 12, because the image resolution is low, only the position and orientation information of the fibers is identifiable, but the boundary information is not clear. Therefore, the visual zoom-in operation is typically required for specifying the interphase of fiber composites. The zoom-in ratio is 4 in this example. The result of the visual zoom-in operation is shown in Figure 14 (b).

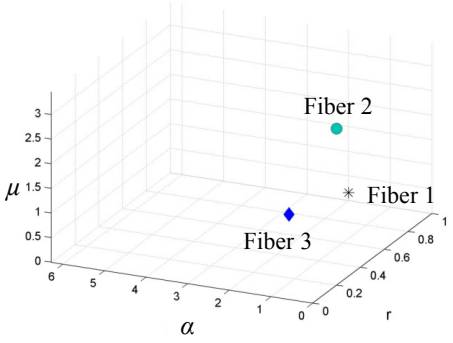

Figure 11 The specification result of locations and orientations of the three fibers in the surfacelet domain at Step 2

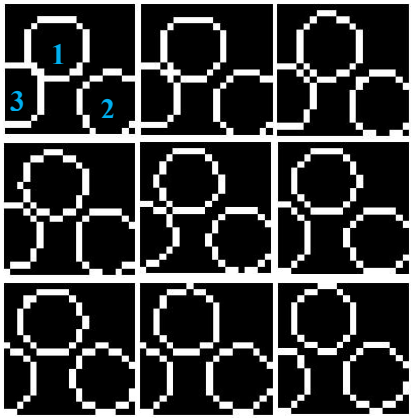

Figure 12 The result of inverse surfacelet transform at STEP 3 (the size of the 3D image is 20×20×9)

In the fourth step, more detailed material microstructural information is specified in the image space. In this example, four additional isosurfaces are specified with two for the interphase region and the other two for the internal region of the fiber. There is no crack or impurity specified in this example. The four additional isosurfaces for Fiber 2 are specified in the image space with four different isovalues of the surfacelet, which are -0.2, -0.1, 0.05 and 0.1 respectively, in order to model the interphase and internal region of Fiber 2. As an example, for the interphase region, the pixel values on the isosurface with the isovalue of 0.03 are set to be 173, and the ones with the isovalue of 0.06 are set to be 32. For the internal region, the pixel values on the two additional isosurface are all set to be 255, assuming a uniform composition inside the fibers. It should be noted that the direct specification of the four additional isosurfaces on the resulting image of Step 3 is technically feasible. However, since the interphase regions are usually thin compared to the radius of the fibers, and one pixel represents a large region in the low-resolution images, it is likely to be inaccurate and inconvenient to specify with

these images. The first slice of the result is shown in Figure 14 (c).

In the fifth step, the forward surfacelet transform is applied so that the surfacelet representation of the material images from Step 4 is obtained. Since the origin of the image space is always in the middle of the 3D image at the current visual scale, the coordinate system is changed during the visual zoom-in operation, and the parameters and all of the coordinates for all five surfacelets are changed. When there is no crack or impurity specified in STEP 4, the new parameters and coordinates of the surfacelets can either be obtained through coordinate system transformation or feature identification in the forward surfacelet transform. In this chapter, to demonstrate the general method, the method of feature identification is utilized. The result is shown in Figure 15. To show the accuracy of the feature identification result, the surfacelets are shown in the image domain by inverse surfacelet transform. The result is shown in Figure 14 (d) for comparison. It can be seen that there is only slight difference between the results in Figure 14 (c) and (d).

In the sixth step, the continuous material distribution model is constructed by interpolating the five collocation points in the surfacelet space for fiber 2 as a result of the previous step. A cubic spline is used in this example.

In the seventh step, the continuous distribution model constructed in the sixth step is evaluated in the surfacelet space. Surface integral values of the surfacelets between the five specified ones in the surfacelet space are predicted with from the cubic spline. The result is shown in Figure 16.

In the last step, the visualization model in the image space is obtained through the inverse surfacelet transform from the evaluation of the distribution model from the seventh step. The pixel values on the same surfacelet are assumed to be the same in this example. When a pixel is on two surfacelets at the same time, the pixel value is the average of the two possible values. The full reconstruction result is shown in Figure 17. Some of the detailed pixel values of the resulting image after the model zoom-in operation in the box region indicated in Figure 17 are listed in Table 1. It is seen that a continuous distribution of materials in the interphase region is obtained.

Table 1 Pixel values of the box region indicated in Figure 17

		Pixel number in the horizontal direction					
		8	***9***	***10***	***11***	***12***	***13***
Pixel number in the vertical direction	***7***	0	0	32	71.4	110.8	173
	8	0	32	71.4	110.9	173	220.4
	9	0	32	110.9	173	220	225
	10	32	110.9	173	220	255	255
	11	110.9	173	220	255	255	255
	12	141.9	220.4	255	255	255	255

Figure 13 The first resulting image of inverse surfacelet transform at Step 3 with enhanced resolution (the size is 50×50×9)

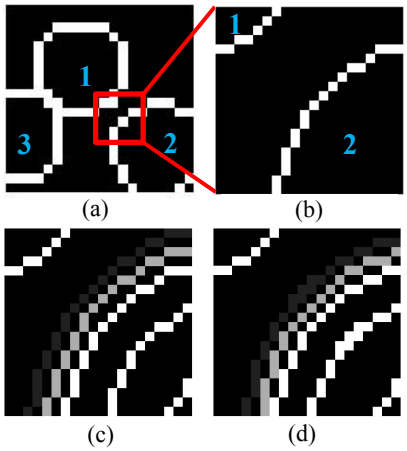

Figure 14 Zoom-in for detailed design of fiber-matrix interphase. (a) The resulting image of STEP 3. (b) The resulting image after visual zoom-in operation. (c) The resulting image of STEP 4. (d) The reconstructed image of the resulting surfacelets in STEP 5.

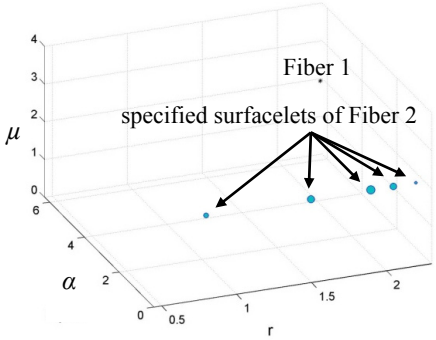

Figure 15 The result of STEP 5

After the specification of the detailed interphase information of Fiber 2, a zoom-out operation can be conducted for the visualization of the overall microstructure. In this example, the image is zoomed out by 4 times of the original visual scale. The surface integral value

at the specified middle collocation point in Figure 15 is used. The result of the zoom-out operation is shown in Figure 18. It is seen that the interphase region has no continuous distribution any more. Suppose that the designer would like to zoom into the interphase region further from the result in Figure 17, the new set of collocation points can be generated either by new specifications in the smaller region from the designer, or by evaluating the distribution model created in the above procedure at the user-specified locations. The new set of collocation points then are used to create the more detailed distribution model, following the same procedure in Figure 1.

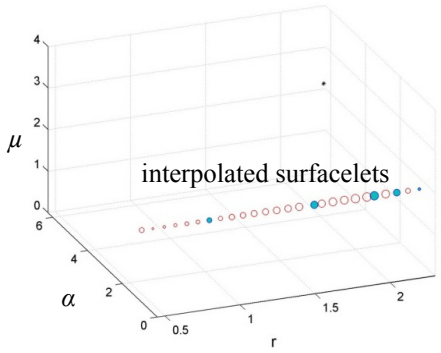

Figure 16 The result of STEP 7

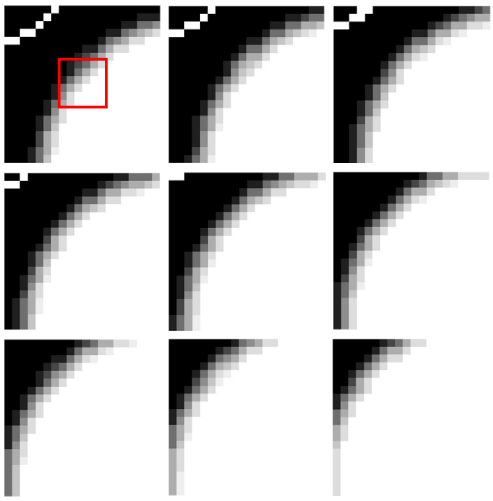

Figure 17 The image reconstruction result in STEP 8

Figure 18 The resulting image of the zoom-out operation (the first slice only)

6. SUMMARY AND FUTURE WORK

In this paper, a materials modeling and specification scheme is proposed for design and visualization of material microstructures at multiple levels of details. The combination of the visual and model zooming mechanisms is able to support seamless zoom-in and zoom-out operations, which are based on a collocation scheme in the surfacelet space. The material distribution is modeled by interpolation of surface integrals in surfacelets. A general specification and modeling scheme is demonstrated with an example of fiber-based composites. The surfacelets created for the main microstructural features at the beginning of the design process can not only be specified by users, but also be obtained from the forward surfacelet transform of existing material images. Therefore, this proposed multi-scale material modeling method also supports the reverse engineering process.

Similar to the material descriptions based on statistical correlations, surfacelet based description is generally incomplete in the sense that the one-to-one mapping between descriptors and original images is not guaranteed, because the dimensionality of descriptors is every high and truncation errors are always involved with the given computational limit. The future extension of this work will include the implementation and test of higher dimensions in the surfacelet domain. To increase flexibility, local deformation and variation of microstructures will also be modeled. With the consideration of process uncertainty, stochasticity or randomness can be introduced into the location and orientation parameters of surfacelets. The sensitivity and robustness of materials properties with respect to the variations need to be assessed. The integrated design process from microstructure specification to material property prediction, e.g. using finite element analysis, will also be demonstrated.

ACKNOWLEDGMENTS

This research was supported in part by the National Science Foundation under the grant No. CMMI-1030385.

REFERENCES

[1] Shan, Z. and Gokhale, A.M., 2004. Digital image analysis and microstructure modeling tools for microstructure sensitive design of materials. *International Journal of Plasticity*, *20*(7), pp.1347-1370.
[2] Lewis, A.C. and Geltmacher, A.B., 2006. Image-based modeling of the response of experimental 3D microstructures to mechanical loading. *Scripta Materialia*, *55*(1), pp.81-85.
[3] Qian, L., Toda, H., Uesugi, K., Kobayashi, M. and Kobayashi, T., 2008. Direct observation and image-based simulation of three-dimensional tortuous crack evolution inside opaque materials. *Physical Review Letters*, *100*(11), 115505.
[4] Corson, P.B., 1974. Correlation functions for predicting properties of heterogeneous materials. I. Experimental measurement of spatial correlation functions in multiphase solids. *Journal of Applied Physics*, *45*(7), pp.3159-3164.
[5] Adams, B. L., Morris, P. R., Wang, T. T., Willden, K. S., & Wright, S. I. (1987). Description of orientation coherence in polycrystalline materials. *Acta Metallurgica*, *35*(12), 2935-2946
[6] Wang, Y., Rosen, D. W., 2010, "Multiscale heterogeneous modeling with surfacelets", Computer-Aided Design and Applications, 7, pp. 759-776.
[7] Huang, W., Wang, Y., Rosen, D. W., 2014, "Inverse Surfacelet Transform for Image Reconstruction with Constrained Conjugate Gradient Methods," Journal of Computing and Information Science in Engineering, 14(2), 021005.
[8] Yang, N., Boselli, J. and Sinclair, I., 2001. Simulation and quantitative assessment of homogeneous and inhomogeneous particle distributions in particulate metal matrix composites. *Journal of Microscopy*, *201*(2), pp.189-200
[9] Ayyar, A. and Chawla, N., 2006. Microstructure-based modeling of crack growth in particle reinforced composites. *Composites Science and technology*, *66*(13), pp.1980-1994.
[10] Valiveti, D.M. and Ghosh, S., 2007. Morphology based domain partitioning of multi-phase materials: a preprocessor for multi-scale modelling. *International Journal for Numerical Methods in Engineering*, *69*(8), pp.1717-1754.
[11] Schröder-Turk, G. E., Mickel, W., Kapfer, S. C., Klatt, M. A., Schaller, F. M., Hoffmann, M. J. F., ... & Reichelsdorfer, M. (2011). Minkowski tensor shape analysis of cellular, granular and porous structures. *Advanced Materials*, *23*(22-23), 2535-2553.
[12] Adams, B. L., Henrie, A., Henrie, B., Lyon, M., Kalidindi, S. R., Garmestani, H., 2001, "Microstructure-sensitive design of a compliant beam," Journal of the Mechanics and Physics of Solids, 49, pp. 1639–1663.
[13] Saheli, G., Garmestani, H., & Adams, B. L., 2004, "Microstructure design of a two phase composite using two-point correlation functions," Journal of Computer-Aided Materials Design, 11(2-3), pp.103-115.
[14] Adams, B. L., Xiang, G., Kalidindi, S. R., 2005, "Finite approximations to the second-order properties closure in single phase polycrystals". Acta Materialia, 53, pp. 3563–3577.
[15] Torquato, S., Beasley, J. D., & Chiew, Y. C. (1988). Two-point cluster function for continuum percolation. *The Journal of chemical physics*, *88*(10), 6540-6547
[16] Manwart, C., Torquato, S., & Hilfer, R. (2000). Stochastic reconstruction of sandstones. *Physical Review E*, *62*(1), 893-899.
[17] Tewari, A., Gokhale, A. M., Spowart, J. E., & Miracle, D. B. (2004). Quantitative characterization of spatial clustering in three-dimensional microstructures using two-point correlation functions. *Acta Materialia*, *52*(2), 307-319
[18] Baniassadi, M., Garmestani, H., Li, D. S., Ahzi, S., Khaleel, M., & Sun, X. (2011). Three-phase solid oxide fuel cell anode microstructure realization using two-point correlation functions. *Acta materialia*, *59*(1), 30-43
[19] Fullwood, D. T., Niezgoda, S. R., Adams, B. L., Kalidindi, S. R., 2010, "Microstructure sensitive design for performance optimization," Progress in Materials Science, 55, pp. 477–562.
[20] Baniassadi, M., Ahzi, S., Garmestani, H., Ruch, D., & Remond, Y. (2012). New approximate solution for N-point correlation functions for heterogeneous materials. *Journal of the Mechanics and Physics of Solids*, *60*(1), 104-119.
[21] Fast, T., Kalidindi, S. R., 2011, "Formulation and calibration of higher-order elastic localization relationships using the MKS approach," Acta Materialia, 59, pp. 4595–4605.
[22] Xu, H., Dikin, D. A., Burkhart, C., & Chen, W. (2014). Descriptor-based methodology for statistical characterization and 3D reconstruction of microstructural materials. *Computational Materials Science*, *85*, 206-216.
[23] Gupta, A., Cecen, A., Goyal, S., Singh, A. K., & Kalidindi, S. R. (2015). Structure–property linkages using a data science approach: Application to a non-metallic inclusion/steel composite system. *Acta Materialia*, *91*, 239-254.
[24] Wu, K., Dijke, M. J., Couples, G. D., Jiang, Z., Ma, J., Sorbie, K. S., Crawford, J., Young, I., Zhang, X., 2006, "3D Stochastic Modelling of Heterogeneous Porous Media – Applications to Reservoir Rocks," *Transport in Porous Media*, 65(3), 443-467.
[25] Wang, Y. (2007). Periodic surface modeling for computer aided nano design. *Computer-Aided Design*, *39*(3), 179-189.
[26] Wang, Y. (2008). Degree elevation and reduction of periodic surfaces. *Computer-Aided Design and Applications*, *5*(6), 841-854.
[27] Wang, Y. (2009). Computing Minkowski Sum of Periodic Surface Models. *Computer-Aided Design and Applications*, *6*(6), 825-837.
[28] Qi, C., & Wang, Y. (2009). Feature-based crystal construction in computer-aided nano-design. *Computer-Aided Design*, *41*(11), 792-800
[29] Huang, W., Didari, S., Wang, Y., & Harris, T. A. (2015). Generalized periodic surface model and its application in designing fibrous porous media. *Engineering computations*, *32*(1), 7-36.

[30] Jung, Y., Chu, K. T., & Torquato, S. (2007). A variational level set approach for surface area minimization of triply-periodic surfaces. *Journal of Computational Physics*, *223*(2), 711-730.
[31] Yoo, D. J. (2011). Porous scaffold design using the distance field and triply periodic minimal surface models. *Biomaterials*, *32*(31), 7741-7754.
[32] Yoo, D. (2013). New paradigms in hierarchical porous scaffold design for tissue engineering. *Materials Science and Engineering: C*, *33*(3), 1759-1772.
[33] Afshar, M., Anaraki, A. P., Montazerian, H., & Kadkhodapour, J. (2016). Additive manufacturing and mechanical characterization of graded porosity scaffolds designed based on triply periodic minimal surface architectures. *Journal of the Mechanical Behavior of Biomedical Materials*, *62*, 481-494
[34] Didari, S., Harris, T. A., Huang, W., Tessier, S. M., & Wang, Y. (2012). Feasibility of periodic surface models to develop gas diffusion layers: A gas permeability study. *International Journal of Hydrogen Energy*, *37*(19), 14427-14438
[35] Yang, N., Gao, L., & Zhou, K. (2015). Simple method to generate and fabricate stochastic porous scaffolds. *Materials Science and Engineering: C*, *56*, 444-450.
[36] Xiao, F., & Yin, X. (2016). Geometry models of porous media based on Voronoi tessellations and their porosity–permeability relations. *Computers & Mathematics with Applications*, *72*(2), 328-348.
[37] Avnir, D., Farin, D., & Pfeifer, P. (1985). Surface geometric irregularity of particulate materials: the fractal approach. *Journal of Colloid and Interface Science*, *103*(1), 112-123.
[38] Mandelbrot, B. B., Passoja, D. E., & Paullay, A. J. (1984). Fractal character of fracture surfaces of metals. *Nature* **308**, 721 - 722
[39] Wang, Y., "3D Fractals from Periodic Surfaces," *2010 ASME International Design Engineering Technical Conferences & The Computer and Information in Engineering Conference (IDETC/CIE2010), Aug. 15-18, 2010, Montreal, Quebec*, Paper No.DETC2010-29081
[40] Huang, W., Wang, Y., & Rosen, D. W. (2016). Material feature representation and identification with composite surfacelets. *Journal of Computational Design and Engineering*, 3(4), 370-384